

## Experimental investigations on factors influencing the calibration of heat flux calorimeters<sup>1</sup>

H.K. Cammenga \* and A.G. Steer

*Institut für Physikalische und Theoretische Chemie, Technische Universität Braunschweig,  
Hans-Sommer-Strasse 10, D-38106 Braunschweig (Germany)*

(Received 28 May 1993; accepted 1 June 1993)

### Abstract

The influences of temperature, heating rate, and of the mass and heat capacity of the sample on the temperature and heat calibration, the time constant and the coefficient of thermal conduction are examined for a power-compensating, MCB-type DSC. The results for a metallic and an organic substance are compared.

### INTRODUCTION

The aim of every calibration is to correlate a measured quantity to the true quantity of interest. To minimize unknown influences, one usually uses identical external conditions in calibration and measurement. This, however, often cannot be realized. In these cases one has to know at least the influences of the changed conditions on the results of the calibration performed. The temperature dependence of the heat and temperature calibration is well known, the latter being also strongly influenced by the heating rate.

The method used in this work was simultaneous temperature and heat calibration using the fusion peaks of organic and metallic substances [1]. A recommendation of the calibration committee of GEFTA (Gesellschaft für Thermische Analyse) for the methods and materials for temperature and heat calibration has recently been published [2–4]. With the exception of cyclopentane, no organic substances were considered; thus one aim here is to compare the behaviour of organic and metallic substances.

### EXPERIMENTAL

The measurements were made in an MCB microcalorimeter, which is connected to a computer. The calorimeter had originally been constructed

---

\* Corresponding author.

<sup>1</sup> Presented at the Tenth Ulm Conference, Ulm, Germany, 17–19 March 1993.

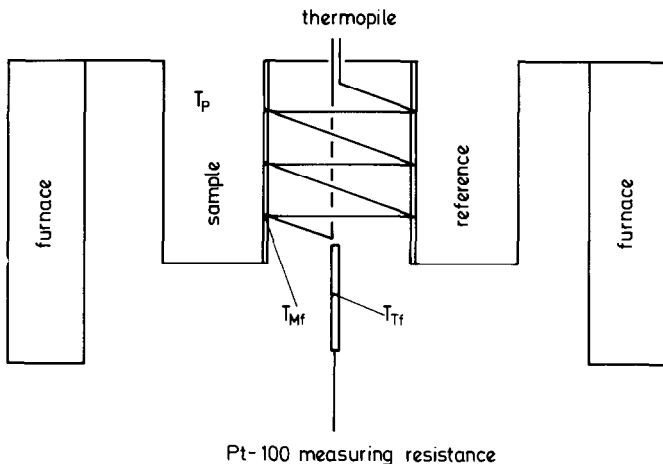


Fig. 1. Temperature measurement within the MCB (schematic):  $T_p$ , temperature of sample;  $T_{Mf}$ , temperature of sensor (connection of thermopile);  $T_{Tr}$ , temperature of Pt resistor.

as a heat flow calorimeter, but now operates in a power-compensating mode. The two cylinders for the sample and the reference have a volume of  $1.5 \text{ cm}^3$  each. The MCB works in the temperature range from 30 to  $400^\circ\text{C}$ . A Pt-100 resistor between the two cells is used for temperature measurement (see Fig. 1). The differential temperature (which is the input signal to the controlling device) is measured by a 70-fold thermopile of NiCr/CuNi. The power necessary to compensate thermal effects is released by two Pt resistors beneath the bottom of each cell. The measuring head is enclosed in a brass cylinder, which is held at a constant temperature of  $20^\circ\text{C}$  by a circulation thermostat.

The samples were sealed in glass ampoules with flat, polished bottoms and a usable volume of approximately  $0.4 \text{ cm}^3$ . After each measurement, the ampoules were removed from the calorimeter, thus minimizing the effect of the positioning of the sample within the oven, the influence of which has been discussed for example in ref. 5. Several measurements were made with each ampoule. The reference was in all cases an empty matched glass ampoule.

For estimating the temperature dependence of the parameters of interest, five substances (organic and metallic) were chosen with melting points in the region between 30 and  $300^\circ\text{C}$  (see Table 1). All materials had a purity of at least 99.9%. The organic substances were purified by vacuum sublimation and zone melting.

The influences of heating rate and sample mass were examined with indium, as an example of a metallic material, and with benzoic acid, as an example of an organic substance. Owing to the high time constant of the MCB (72 s), only low heating rates could be applied for a reasonable

TABLE 1

Selected calibration materials

Material	$\theta_{\text{fus}}/^{\circ}\text{C}$	$\Delta_{\text{fus}}H/\text{kJ mol}^{-1}$	Ref.
Gallium	29.772	5.586	6, 7
Biphenyl	69.2	18.58	6, 8
Benzoic acid	122.4	18.00	9
Indium	156.634	3.282	6, 10
Tin	231.97	7.195	6, 11

temperature resolution; thus the heating rate was varied in the range  $0.01\text{--}1\text{ K min}^{-1}$ . The mass of the samples was varied up to 162 mg, which is equivalent to a heat capacity of  $0.25\text{ J K}^{-1}$ . The absolute enthalpies of fusion were in the range  $0.98\text{--}18.27\text{ J}$ .

The influences of the parameters of interest on the temperature correction  $\Delta T$ , the heat calibration factor  $E$ , the signal time constant  $\tau_{\text{sig}}$ , and the coefficient of thermal conduction  $S$  were examined. All these quantities were evaluated from the melting peak using a program originally developed by Reichelt [12]. The starting and ending points of the peak were set by eye.

## THEORY

The quantities of interest represented in Fig. 2 from each fusion peak were evaluated as follows:

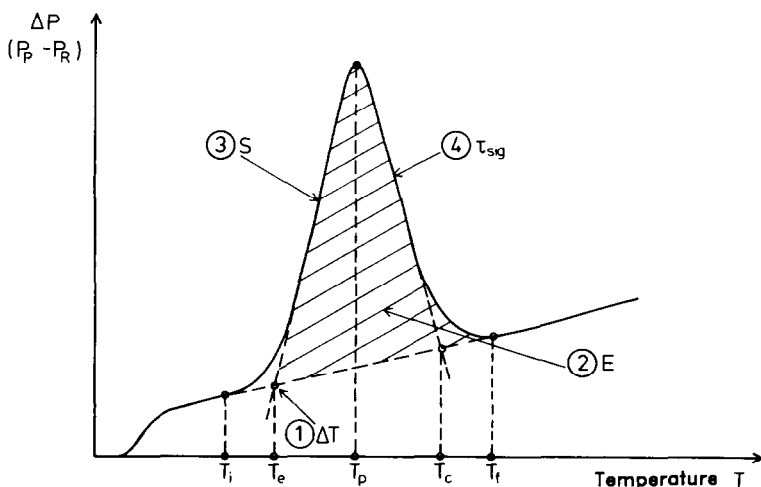


Fig. 2. Evaluation of different quantities from a fusion peak:  $P_p$ , power released into sample cell;  $P_R$ , power released into reference cell;  $T_e$ , extrapolated peak onset temperature.

1. The temperature correction  $\Delta T$  is estimated, according to the GEFTA recommendation [2], as the difference between the known melting temperature of the substance  $T_{\text{fus}}(\theta_{\text{fus}})$  and the extrapolated onset temperature  $T_e(\theta_{\text{on}})$ . The onset temperature is the temperature of the intersection of the extrapolated baseline and the tangent to the DSC curve at the point of inflection

$$\Delta T = T_{\text{fus}} - T_e = \theta_{\text{fus}} - \theta_{\text{on}} \quad (1)$$

2. The heat calibration factor  $E$  is the ratio of the measured amount of heat  $Q_{\text{meas}}$  (peak area) and the true heat consumption  $Q_{\text{true}}$

$$E = \frac{Q_{\text{meas}}}{Q_{\text{true}}} \quad (2)$$

The baseline in the region of the peak area was constructed as a straight line between  $T_i$  and  $T_f$ . This is sufficient owing to the sharp peak and the small difference in the baseline before and after the peak (small change in heat capacity).

The heat calibration factor  $E_Q$  is not equal to the heat flow calibration factor  $E_\Phi$ , but because the difference is in the region of 1% for power-compensating DSCs,  $E_\Phi$  was not determined separately, e.g. by electrical calibration or by heating of a reference substance with known heat capacity.

3. The location of the sample and of the differential temperature measurement are separated by a heat conduction path with a thermal resistance  $R$ . The reciprocal of this thermal resistance  $R$  is the coefficient of thermal conduction  $S$ , which can be calculated from the slope of the rising part of the peak

$$S = \frac{1}{R} \approx \frac{(d \Delta P / dt)}{\beta} \quad (3)$$

where  $d \Delta P / dt$  is the change in power with respect to time, and  $\beta$  is the heating rate.

4. The signal time constant  $\tau_{\text{sig}}$  can be determined from the descending part of the melting peak, which is approximately describable by an exponential function;  $\tau$  represents the delayed detection of a thermal event occurring in the sample by the measuring system. The time constant depends on the thermal resistance and the heat capacity of the measuring system and the sample

$$\Delta P = \text{const} \cdot \exp\left(-\frac{t}{\tau_{\text{sig}}}\right) \quad (4)$$

$$\tau_{\text{sig}} = C_p R \quad (5)$$

where  $\Delta P$  is the differential power,  $t$  the time, and  $C_p$  the heat capacity of measuring system and sample.

In the MCB calorimeter, the location of the temperature measurement is neither that of the sample nor that of the differential temperature measurement (see Fig. 1). Therefore the temperature of the sample  $T_p$  has to be calculated from the measured temperature  $T_{Tr}$

$$T_p = T_{Tr} - \tau_{lag}\beta - R \frac{dQ}{dt} \quad (6)$$

where  $\tau_{lag}$  is the furnace time constant and  $dQ/dt$  the rate of heat release/consumption.

## RESULTS AND DISCUSSION

The temperature correction  $\Delta T$  lies within  $\pm 0.5$  K in the temperature region examined (see Fig. 3(a)), with a maximum at about  $100^\circ\text{C}$ . At higher temperatures the correction becomes negative, due to rising heat losses by radiation.

$\Delta T$  decreases linearly with the heating rate, see Fig. 3(b). In ref. 5, a linear correlation was observed for heating rates up to  $160 \text{ K min}^{-1}$  for another power-compensated DSC.

The slope of the fitted curve represents the furnace time constant  $\tau_{lag}$ , which describes the lag of the sample temperature behind the furnace temperature due to the dynamic conditions. For benzoic acid and indium, one obtains almost the same values of 30.5 and 33.5 s, respectively. In the case of large masses, temperature gradients occur within the sample, which seems to melt at apparently higher temperatures. For indium, this is true to a less degree, but for benzoic acid the temperature correction is independent of the sample mass (Fig. 3(c)). A precise temperature calibration is especially important for kinetic investigations.

Because of increasing heat losses, one would expect the heat calibration factor  $E$  to increase with rising temperature. But the opposite seems to be the case, although the scatter of the data is too large to make a clear statement.  $E$ , however, is independent of the kind of material (metallic or organic) used (Fig. 4(a)).

For indium,  $E$  decreases with increasing heating rate, see Fig. 4(b), which is in accordance with theoretical considerations [13]. For benzoic acid, there is again a large scatter in the results, but overall  $E$  seems to be independent of the heating rate.

The effect of sample mass is much less pronounced (Fig. 4(c)), but  $E$  seems to increase slightly with increasing mass and heat capacity.

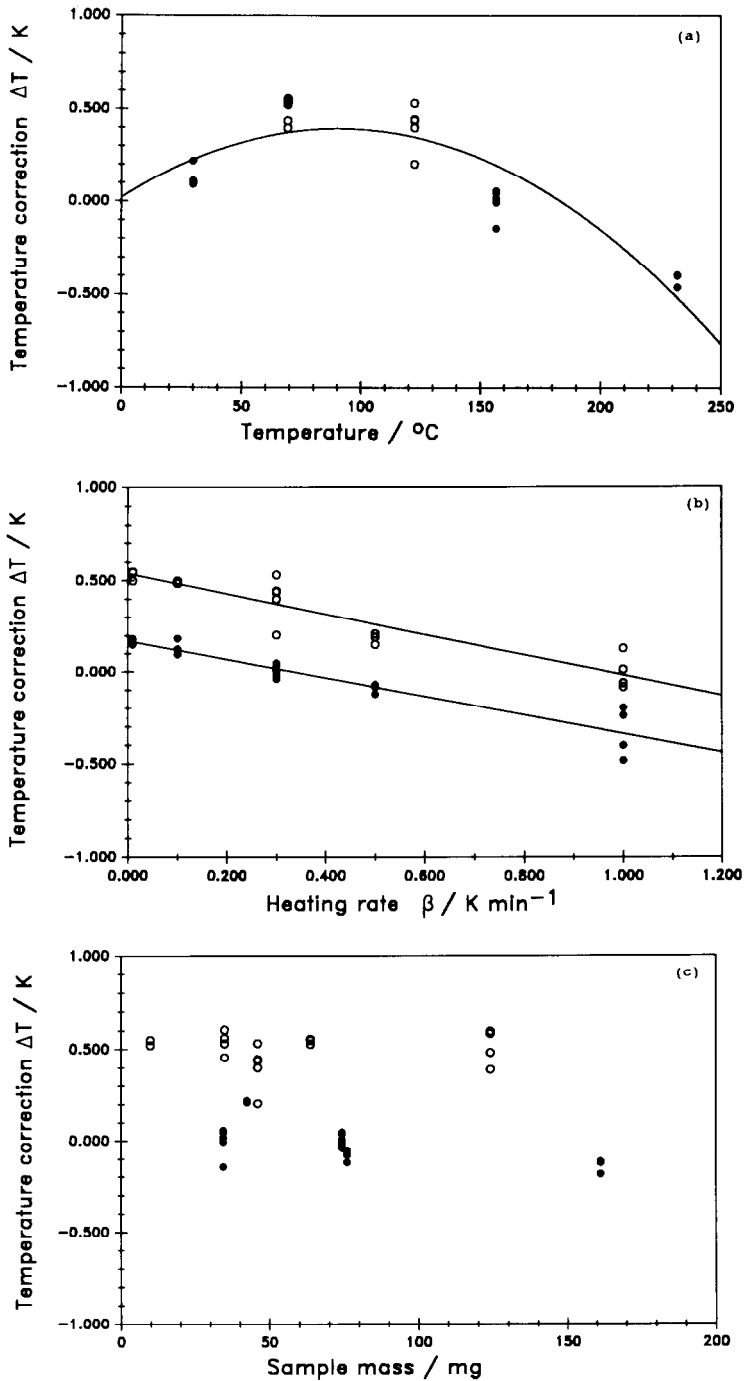


Fig. 3. Temperature correction determined by fusion experiments. (a) Influence of temperature:  $\beta = 0.3 \text{ K min}^{-1}$ ; sample mass, about 30 mg. (b) Influence of heating rate: ●, indium (74.30 mg); ○, benzoic acid (46.02 mg). (c) Influence of sample mass: ●, indium; ○, benzoic acid;  $\beta = 0.3 \text{ K min}^{-1}$

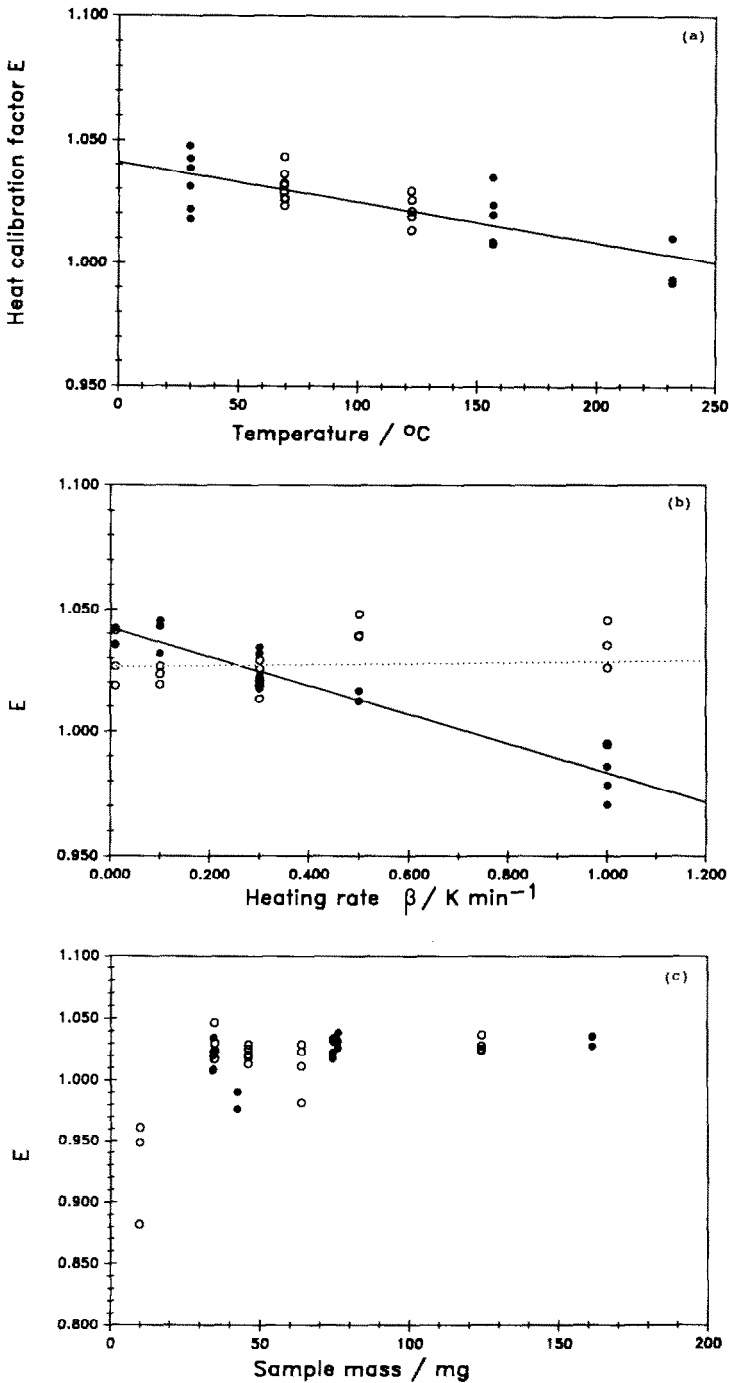


Fig. 4. Heat calibration factor  $E$  determined by fusion experiments. (a) Influence of temperature:  $\beta = 0.3 \text{ K min}^{-1}$ , sample mass, about 30 mg. (b) Influence of heating rate: ●, indium (74.30 mg); ○, benzoic acid (46.02 mg). (c) Influence of sample mass: ●, indium; ○, benzoic acid;  $\beta = 0.3 \text{ K min}^{-1}$ .

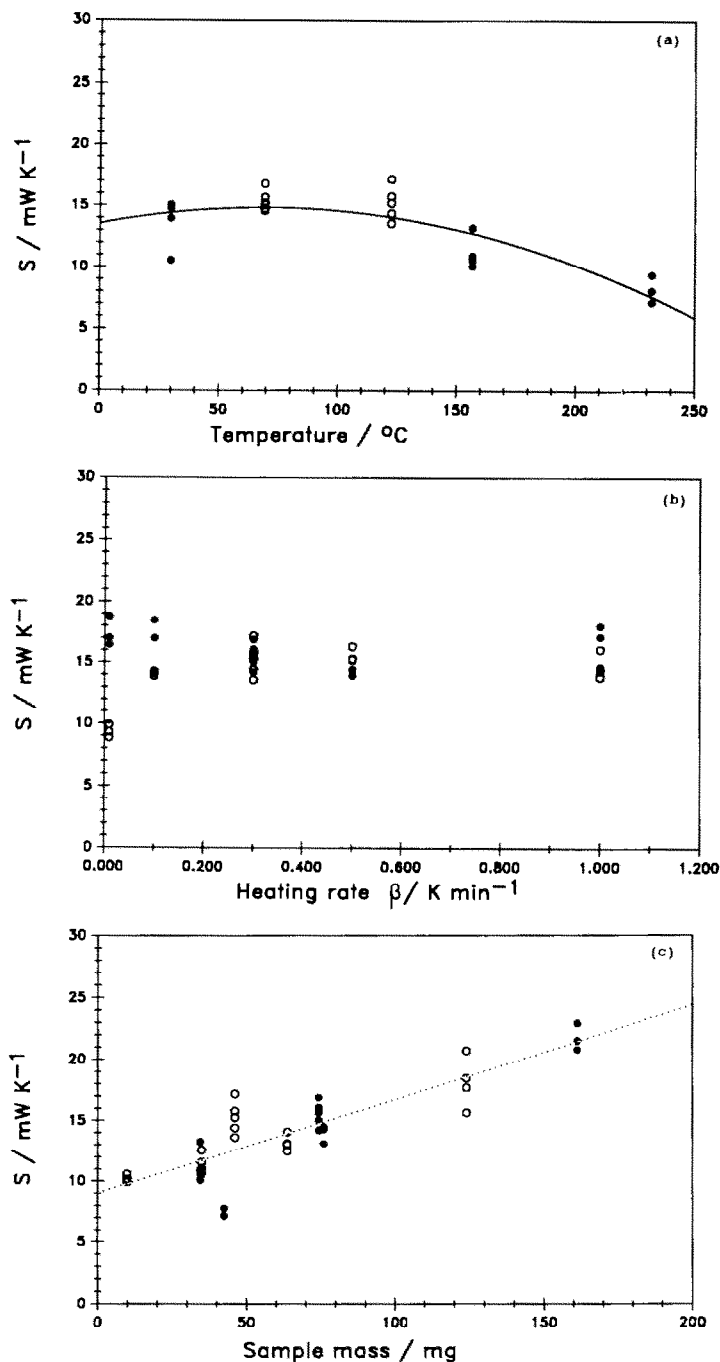


Fig. 5. Coefficient of thermal conduction  $S$  determined by fusion experiments. (a) Influence of temperature:  $\beta = 0.3 \text{ K min}^{-1}$ ; sample mass, about 30 mg. (b) Influence of heating rate:  $\bullet$ , indium (74.30 mg);  $\circ$ , benzoic acid (46.02 mg). (c) Influence of sample mass:  $\bullet$ , indium;  $\circ$ , benzoic acid;  $\beta = 0.3 \text{ K min}^{-1}$ . (d) Influence of sample heat capacity:  $\bullet$ , indium;  $\circ$ , benzoic acid;  $\beta = 0.3 \text{ K min}^{-1}$ .



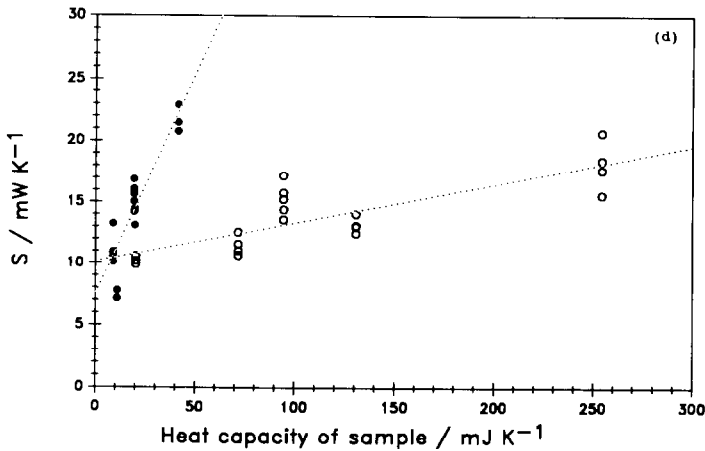


Fig. 5 (continued)

Obviously, to a first approximation,  $S$  is not dependent on the heat conductivity  $\lambda$  of the sample because similar values are obtained for the metallic and the organic substances.  $S$  is independent of the heating rate, but increases linearly with the mass and heat capacity of the sample for indium and benzoic acid. This is probably due to an increasingly better contact between the sample and the glass surface. The dependence on sample heat capacity is much stronger for indium than for benzoic acid (Fig. 5(a)–(d)).

The time constant  $\tau_{\text{sig}}$  is independent of temperature, although the scatter is relatively large (Fig. 6(a));  $\tau_{\text{sig}}$  seems to decrease slightly with increasing heating rate (Fig. 6(b)). In eqn. (5),  $C_p$  represents the sum of the heat capacities of the system and of the sample; thus  $\tau_{\text{sig}}$  increases with increasingly sample mass. An extrapolation to  $C_p(\text{sample}) \rightarrow 0$  should yield a kind of system heat capacity, which can be estimated as 30–40 s for the MCB microcalorimeter (Fig. 6(c) and (d)).

The results are summarized in Table 2. As one can see, the temperature and the heating rate are the main influencing factors. The behaviour of indium and benzoic acid differs only with respect to the influence of the heating rate  $\beta$  on the heat calibration factor  $E$ ; thus organic substances seem to be just as suitable as metallic ones for calibration.

Measurements have also been made with some “older” samples. These samples had been used before and had been stored for a few years in sealed glass measuring ampoules. With the exception of tin, no significantly different results were obtained. Nevertheless, one should not use calibration samples for too long a period, because metals may oxidize and organic substances could decompose.

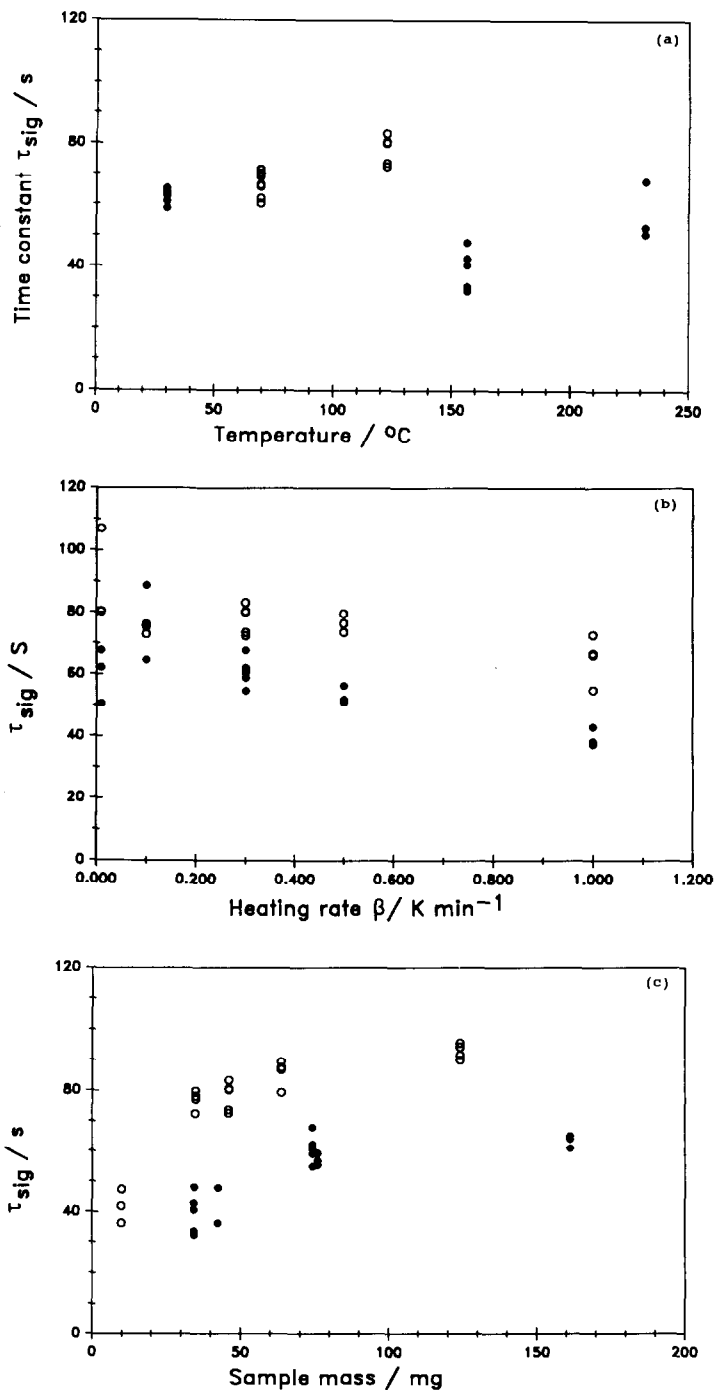


Fig. 6. Time constant  $\tau_{sig}$  determined by fusion experiments. (a) Influence of temperature:  $\beta = 0.3 \text{ K min}^{-1}$ ; sample mass, about 30 mg. (b) Influence of heating rate: ●, indium (74.30 mg); ○, benzoic acid (46.02 mg). (c) Influence of sample mass: ●, indium; ○, benzoic acid;  $\beta = 0.3 \text{ K min}^{-1}$ . (d) Influence of sample heat capacity; ●, indium; ○, benzoic acid;  $\beta = 0.3 \text{ K min}^{-1}$ .

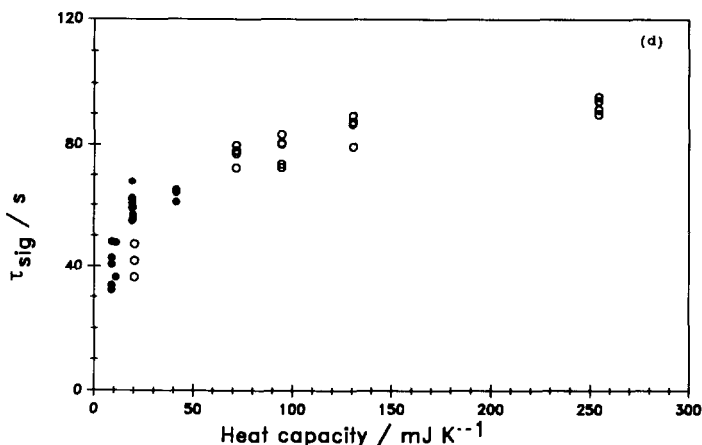


Fig. 6 (continued)

TABLE 2

The correlation between the investigated parameters and the results of the calibration

	Temperature $\theta$	Heating rate $\beta$		Mass $m$ and heat capacity $C_p$	
		BA	In	BA	In
$\Delta T$	2	-1	-1	0	0
$E$	-1	0	-1	0	0
$S$	2	0	0	1	1
$\tau_{\text{sig}}$	0	-1	-1	+	+

Key: BA, benzoic acid; In, Indium; 0, independent; 1, linear correlation; 2, describable by second-order orthogonal polynomial; +, increasing; -, decreasing.

## REFERENCES

- 1 S. Sarge and H.K. Cammenga, *Thermochim. Acta*, 94 (1985) 17–31.
- 2 G.W.H. Höhne, H.K. Cammenga, W. Eysel, E. Gmelin and W. Hemminger, *Thermochim. Acta*, 160 (1990) 1–12.
- 3 H.K. Cammenga, W. Eysel, E. Gmelin, W. Hemminger, G.W.H. Höhne and S.M. Sarge, *PTB Mitt.*, 102 (1992) 13–18.
- 4 S.M. Sarge, E. Gmelin, G.W.H. Höhne, H.K. Cammenga, W. Hemminger and W. Eysel, publication in preparation.
- 5 G.W.H. Höhne and E. Glögler, *Thermochim. Acta*, 151 (1989) 295–304.
- 6 U. Schley, *PTB Mitt.*, 89 (1979) 13–21.
- 7 G.B. Adams, H.L. Johnston and E.C. Kerr, *J. Am. Chem. Soc.*, 74 (1952) 4784–4787.
- 8 K. Ueberreiter and H.-J. Orthmann, *Z. Naturforsch. Teil A*, 5 (1950) 101–108.
- 9 G.T. Furukawa, R.E. McCoskey and G.J. King, *J. Res. Natl. Bur. Stand.*, 47 (1951) 256–261.
- 10 F. Grønvold, *J. Therm. Anal.*, 13 (1978) 419–428.
- 11 F. Grønvold, *Rev. Chim. Miner.*, 11 (1974) 568–584.
- 12 J. Reichelt, Dissertation Technical University of Brunswick, Germany, 1985.
- 13 G.W.H. Höhne, *Thermochim Acta*, 69 (1983) 175–197.